

RHIC Beam Use Request for Run17

The RHICf Collaboration

May 27, 2016

Contents

1	Executive Summary	1
2	Physics Targets	2
2.1	Cross section measurements of forward neutral particle production for cosmic-ray physics	2
2.2	Single-spin asymmetry measurements of the very forward neutral particle production	4
3	Experimental Setup	4
3.1	Installation at the STAR forward region	4
3.2	Data acquisition	7
4	Run17 Request	8
4.1	Beam parameters	8
4.2	Data taking time and statistics	10
4.2.1	Cross section measurements	11
4.2.2	Asymmetry measurements	15
4.2.3	Backup plan of the asymmetry measurements	17
4.2.4	Summary	17
4.3	Joint analysis with STAR	18
4.4	Beam setup time and contingency	18

1 Executive Summary

RHICf requests 4 days of beam time in Run17 with $\sqrt{s}=510$ GeV radially polarized p+p collisions, including beam setup time for the RHICf dedicated optics and moderate contingency. Requested parameters are summarized in Tab.4.1. Notable parameters are $\beta^*=10$ m and radial polarization. According to the CA-D estimation in "RHIC Collider Projections (FY2014–FY2018)", setup time to large β^* collisions is 1 day assuming the previous beam

energy is 255 GeV. Setup to the radial polarization requires additional 1-3 shifts, meaning another 1 day. Because RHICf can accomplish the two physics goals in parallel with 12 hours of data taking, 2 days (48 hours) are requested to complete physics including beam down time and moderate contingency. When, and only when 24 hours of data taking is not achieved after 4 days, RHICf requests another day of data taking, meaning optional 5th day.

2 Physics Targets

RHICf has two physics targets. Because the background of each topic was already described in the Letter of Intent [1] and Proposal [2], the advantages of the RHICf measurements are stresses below.

2.1 Cross section measurements of forward neutral particle production for cosmic-ray physics

Cross sections of forward particle production in hadronic collisions are crucial in modeling the development of atmospheric air showers produced by high-energy cosmic rays. The Large Hadron Collider forward (LHCf) experiment [3] has so far measured cross sections of π^0 s (and their decayed photons) and neutrons at LHC hadron collisions, covering \sqrt{s} from 900 GeV to 13 TeV [4]. To interpolate and extrapolate the knowledge from the accelerator measurements in the air shower modeling, scaling or scaling violation of cross sections in \sqrt{s} is a key point.

LHCf measurements shown in Fig.1 indicate the Feynman scaling in π^0 cross sections between $\sqrt{s}=2.76$ TeV and $\sqrt{s}=7$ TeV [5]. One of the physics targets of the RHICf experiment is to extend this measurements in more wider \sqrt{s} . Fig.2 shows the π^0 cross sections predicted by the EPOS-LHC model [6] at $\sqrt{s}=510$ GeV, 7 TeV, and 100 TeV. In this interval (factor 13–14 each step), the model predicts 20% reduction of cross section at each step. The target uncertainty of the cross section measurement to compare with the LHCf data is 5%. In the LHCf data, total error of the cross section determination at mid- x_F is so far 8%. The dominant source of this error is uncertainty in the energy scale, that was determined from the difference between the π^0 rest mass and the measured peak in the photon-pair invariant mass corresponding to π^0 . Because LHCf recently understood the reason of this difference and developed a correction method, this 8% error used in the 7 TeV data analyses will be reduced from the next analysis. In the analysis of 13 TeV data, the difference is already reduced within the known systematic uncertainty of the energy calibration. Known uncertainty, $\pm 3.5\%$, in the energy scale results 3% uncertainty in cross section.

Advantage of RHICf is main detector response have been already tested at the beam test in the CERN North Area facility [7], where hadron and electron beams from 50–350 GeV, completely overlapping with the RHIC energy, are available.

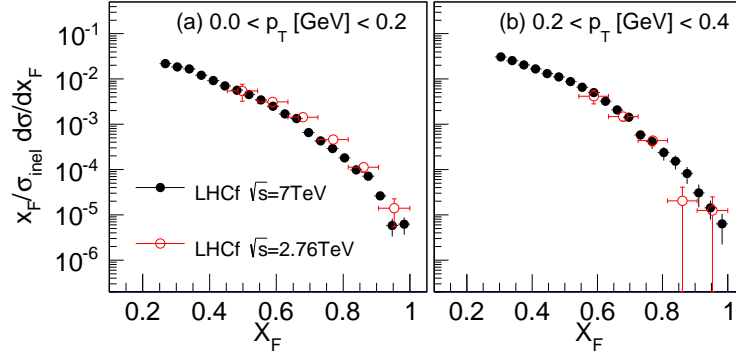


Figure 1: π^0 spectra as a function of x_F measured by LHCf at $\sqrt{s}=2.76$ and 7 TeV [5].

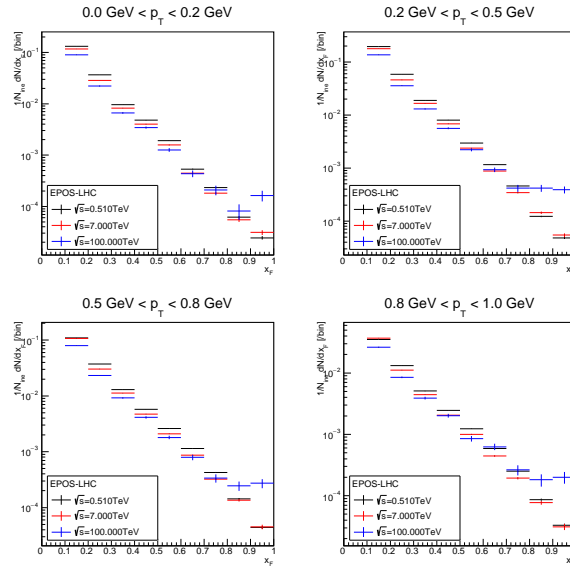


Figure 2: π^0 production yields at $\sqrt{s}=0.51, 7,$ and 100 TeV predicted by the EPOS-LHC generator.

To achieve $<5\%$ total uncertainty, statistical uncertainty is requested to be at the 1% level or less, meaning the number of events in each measurement unit (bin) must be more than 10^4 . Total 5% error is challenging, but a possible target.

2.2 Single-spin asymmetry measurements of the very forward neutral particle production

Origin of the single-spin asymmetry in the polarized proton beam collisions is related to the nature of the pion and Reggeon exchanges [8]. PHENIX measured a p_T scaling of asymmetry amplitude A_N as shown in Fig.3 [9]. However, because the different p_T ranges were covered by different \sqrt{s} data, scaling can be held in \sqrt{s} . To resolve this situation, A_N measurements at a few p_T points below 0.3 GeV and extension of the measurements above 0.3 GeV in a single \sqrt{s} condition are necessary.

The PHENIX measurements in the low p_T range were limited due to the position resolution of the detector. The particle incident position in the Zero Degree Calorimeter [10] (ZDC) used in the measurements was determined by the Shower Maximum Detector (SMD) inserted in the ZDC. Because of the 10 mm strip size in SMD, the position resolution for the neutron incident was limited to 10 mm. Analysis close to the zero degree, small p_T , was limited by this resolution. The high p_T reach was limited by the size of the detector because the performance of the ZDC deteriorates near the edge.

RHICf can improve in both limitations. Because of the fine position resolution, ~ 1 mm, of the RHICf detector for hadronic showers [11], events near the zero degree can be also included in analysis, then the sensitivity to very low p_T is improved. Position resolution was confirmed using the 150 GeV proton beam at the CERN SPS North Area facility [11]. The RHICf detector can vertically move using a manipulator. Although the physical sizes of the RHICf calorimeters are smaller than ZDC, effective acceptance from zero degree is extended. The highest accessible p_T is limited by the projection of the beam pipe between IP and the detector.

3 Experimental Setup

3.1 Installation at the STAR forward region

RHICf uses the former LHCf Arm1 detector [12] as shown in Fig.4. The detector consists of two compact sampling calorimeters with the dimensions transverse to the beam direction $20\text{ mm} \times 20\text{ mm}$ and $40\text{ mm} \times 40\text{ mm}$, and longitudinal size of 250 mm composed of 44 radiation lengths of Tungsten. Sixteen sampling layers every 2 or 4 radiation lengths, and four position sensitive layers composed of GSO bar hodoscope [13] are inserted at 6, 10, 30, and 42 radiation lengths. The RHICf calorimeters can measure

- photons (electromagnetic showers) with energy and position resolutions $<5\%$ and $<200\ \mu\text{m}$, respectively above 100 GeV.

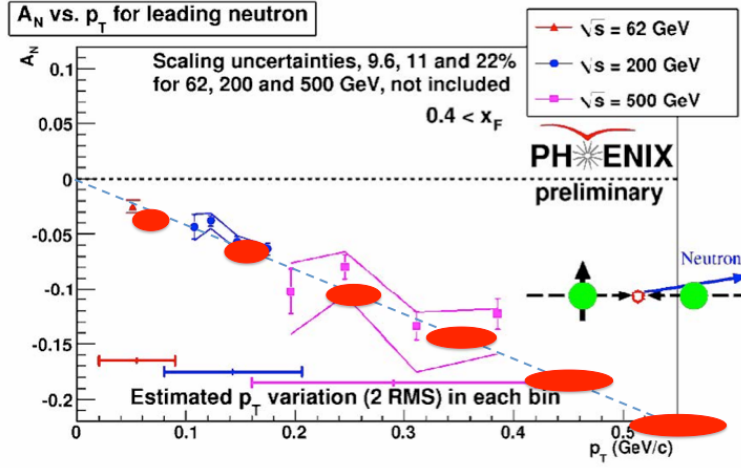


Figure 3: Single spin asymmetry of forward neutron production measured by PHENIX [9]. Red ellipses are expected results from the RHICf experiment.

- neutrons (hadronic showers) with energy and position resolutions $\sim 40\%$ and < 1.2 mm, respectively above 100 GeV.
- π^0 's by identifying photon pairs in two calorimeters simultaneously.

The detector and electronics were shipped out from CERN in the end of April 2016, and arrived at BNL in early May.

The RHICf detector will be installed in front of the ZDC, 18 m West from the STAR interaction point. At this location, two beam pipes have 10 cm gap allowing insertion of the RHICf detector. In the longitudinal direction, to allow the RHICf installation, the ZDC will be moved back several centimeters. In the vertical direction, the space is limited by a radiation shield. To allow the installation of the RHICf detector and its vertical movement, the slot of the shield will be expanded during summer shutdown in 2016. Fig.5 shows the RHICf installation in the forward region of the STAR interaction point.

Fig.6 shows the beam pipe structure between the DX magnet and the RHICf installation location. The narrowest 12 mm gap between two pipes at 16 m from IP limits the horizontal aperture of the RHICf measurement. Fig.7 shows the cross section of the RHICf detector viewed from IP. The area obscured by the two beam pipes (shadow) is indicated by the grey shaded area. A circle with dashed line shows the limit given by the single pipe between the DX magnet and IP. The edges of the two calorimeters are indicated by two red squares, where the center of the small calorimeter is placed at the beam center marked by a cross

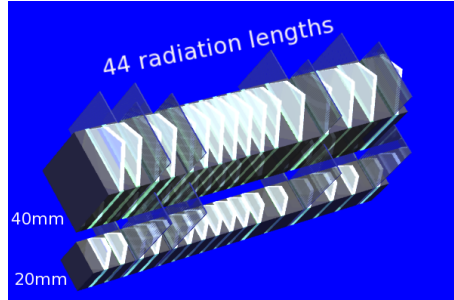


Figure 4: Schematic views of the RHICf detector.

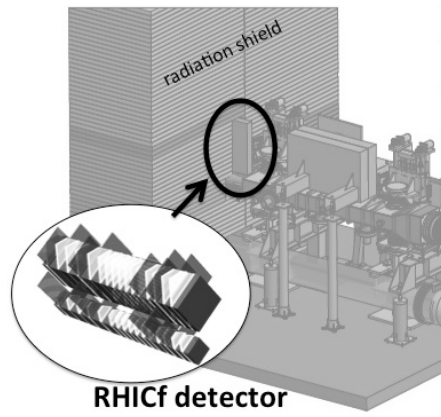


Figure 5: Installation of the RHICf detector in the forward region of STAR interaction point.

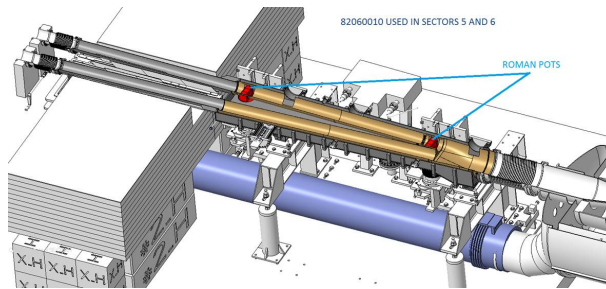


Figure 6: Beam pipe structure between the DX magnet and the RHICf location.

assuming no beam crossing angle. Here the *beam center*, or neutral center, is defined as the projection of the beam direction at the IP to the RHICf detector position. Vertical 0 mm is defined as the vertical position of the non-crossing beam center. The area indicated in blue shows the effective aperture of the RHICf calorimeters for photon measurements, while blue plus light blue shows the aperture for neutron measurements. This difference is because the thickness of the beam pipe is sufficient to obscure photons, but not for hadrons.

The detector will be held by a manipulator that moves the detector vertically by remote control. Definition of the other possible detector positions are shown in Fig.8. These positions are assumed in Sec.4.2 to estimate the total operation time and statistics. Another position, *garage*, is also defined so that the RHICf detector does not interfere the operation of the ZDC.

3.2 Data acquisition

Each PMT signal from 32 sampling scintillators is fed to a discriminator and generates *hit* signal when the pulse height exceeds a predefined threshold level. A shower trigger is issued when any 3 successive layers generate hits and when the timing is synchronized with a passage of a bunch directing to the RHICf detector. The hit signals are handled by a FPGA module, there is flexibility in the event trigger. Possible options to be used are two photon trigger with one photon in each calorimeter to enhance π^0 events, deep (shallow) shower trigger to enhance photon (hadron) events. Because of the transfer speed of the VME system, the maximum data recording rate is limited to 1 kHz. Prescaling for events with large cross sections will be applied. More detailed description of the LHCf trigger is described in [14].

The trigger signal of the RHICf experiment is sent to STAR and STAR records its signal accordingly. Once STAR accepts to record a RHICf trigger, STAR sends back a *token* of the event for RHICf to identify the common event at the offline analysis. Preparation for this data exchange is ongoing.

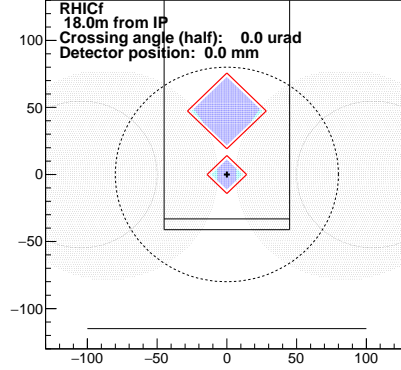


Figure 7: RHICf cross section viewed from IP. This configuration is defined as position-1. Rectangle shown by solid line indicates the envelope of the RHICf detector. Two red squares and blue+light blue hatched area show two calorimeters and effective area, respectively. Grey hatched area and a big dashed circle show the apertures limited by the two beam pipes and the single beam pipe, respectively. The cross indicates the projection of the beam direction, zero degree.

4 Run17 Request

4.1 Beam parameters

The required beam parameters are summarized in Tab.4.1. The major differences from the usual RHIC operation are a large β^* , 10 m, to allow more parallel collisions, and a radial polarization to maximize the single-spin asymmetry in the vertical direction.

With these beam parameters, the expected maximum luminosity will be $3.0 \times 10^{31} \text{ cm}^{-2} \text{ s}^{-1}$. As an average luminosity, we assume $2.0 \times 10^{31} \text{ cm}^{-2} \text{ s}^{-1}$ in the following estimation. With this luminosity and the inelastic cross section $\sigma_{ine} = 50 \text{ mb}$, average interaction rate is 1 MHz. Under this condition, collision pile-up μ is 0.127. When RHICf observes a particle in any of the calorimeters, the probability there is another particle originated from another collision is $0.127 \times 0.018 = 0.2\%$. (Here 0.018 is the RHICf event rate per collision as explained in Sec.4.2.) Because this multi-hit due to collision pileup is at an acceptable level, this highest luminosity condition is used for the RHICf stand-alone physics. However, to identify common collision events with STAR, $\mu = 0.127$ is not ideal. For joint analysis, we need low luminosity run by tuning the luminosity with beam separation.

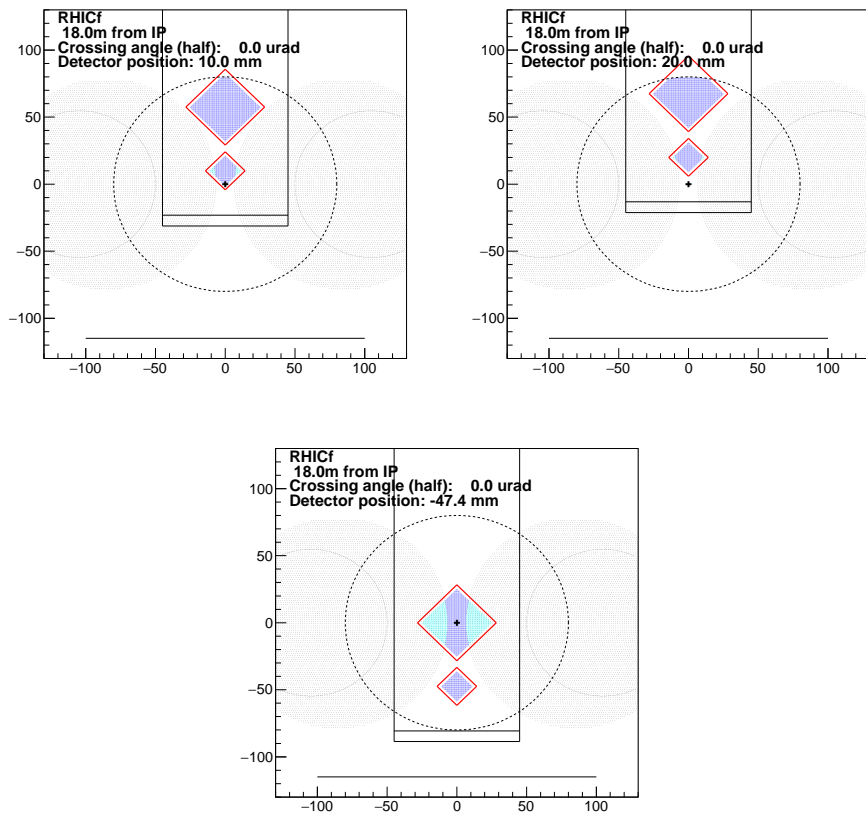


Figure 8: Definition of the various vertical detector positions. Position-2: 10 mm above the beam center. Position-3: 20 mm above the beam center. Position-4: 47.4mm below the beam center where the large calorimeter covers the beam center.

Table 1: Required beam parameters for 510 GeV p+p collision.

Parameter	Value
Beam energy (GeV)	255
Beam intensity (protons per bunch)	2×10^{11}
Number of colliding bunch	111
Number of non-colliding bunch	9
Beam emittance (mm mrad)	20
β^* (m)	10
Luminosity ($\text{cm}^{-2}\text{s}^{-1}$)	2.0×10^{31}
Polarization direction	radial
Polarization amplitude	0.4–0.5
β^* setup time	1 day
Radial polarization setup time	1 day
Data taking time	2 days

4.2 Data taking time and statistics

As explained in Sec.3.2, the DAQ speed of RHICf is limited to 1 kHz. A brief summary of the RHICf trigger and luminosity optimization are

- Trigger is issued when a shower trigger is issued from any of two calorimeters (single event).
- Single events are recorded after prescaling to enhance the photon pair events explained below.
- When a pair of (photon) showers, one in each calorimeter, is observed, the event (pair event) is recorded without prescaling. Pairs are predominantly produced by decay of π^0 and these events are classified as Type I π^0 .
- When a photon pair hits a single calorimeter (Type II π^0), this is recorded as a single event.
- Luminosity is optimized to collect enough statistics of Type I π^0 unless pileup affects the measurement of single events as discussed in Sec.4.1.

Acceptances defined as trigger per inelastic collision for each category of event and the detector position are summarized in Tab.2. In this calculation, EPOS-LHC interaction model was used as an event generator and 70% detection efficiency was applied to the

Table 2: Acceptance (trigger per collision) for each category of the event and the detector positions. "high-E γ " means a trigger condition set only to trigger photons with $E > 100$ GeV.

Position	Acceptance (10^{-2} triggers per collision)			
	Single (all)	Single (photon)	Single (neutron)	Type I π^0
1 (0 mm)	1.83	1.06	0.77	5.7×10^{-3}
2 (10 mm)	1.49	0.86	0.64	5.6×10^{-3}
3 (20 mm)	1.03	0.57	0.46	4.7×10^{-3}
4 (-47.4 mm)	2.25	0.81	1.45	3.1×10^{-3}
0 (0 mm) high-E γ	0.05	0.05	0.00	–

neutron detection. Threshold energies for photons and neutrons were assumed to be 20 GeV and 60 GeV, respectively. In case of the detector position-1, when the small calorimeter covers the beam center, the acceptance of the single events is 1.8%. Assuming the maximum luminosity $2.0 \times 10^{31} \text{ cm}^{-2} \text{ s}^{-1}$ and interaction rate 1 MHz, the expected trigger rate for the single event is 18 kHz. To limit the actual recording rate to 800 Hz, the prescaling factor for single events will be 0.044 while no reduction is applied for the photon pair events.

4.2.1 Cross section measurements

Under these conditions and $L = 2.0 \times 10^{31}$, effective operation time to achieve 10^8 inelastic collisions are 2,300 sec and 100 sec for single and pair events, respectively. Or, within 1 hour of operation RHICf can collect events equivalent to 1.6×10^8 and 3.6×10^9 inelastic collisions for single and pair events, respectively. The expected observed spectra after 1 hour of operation are shown in Fig.9 and Fig.10. In some energy and p_T regions, number of single events exceeds 10^4 in 10 GeV binning.

Fig.11 and Fig.12 show the expected combined spectra observed at positions- 1, 2, and 3, assuming 4 hours of operation at each detector position (total 12 hours). Here, same prescaling factor 0.044 was applied to the single event trigger at three positions. For the single neutron events, in most of the energy and p_T regions, more than $10^4/10$ GeV bin can be recorded. This is a minimal goal of the cross section measurement.

To increase the high energy, high p_T photons, high-threshold operation is effective. By setting the shower recognition pattern, the trigger to electromagnetic showers can be enhanced. By increasing the threshold to 100 GeV, single photon events can be recorded without prescaling. Fig.13 shows the expected spectra observed with the high-energy photon trigger at three detector positions assuming one hour at each position. About 10^3 events/10 GeV bin can be observed even in the high-energy and high p_T region.

Table 3: Trigger and recording (DAQ) efficiencies for different category of events when $L=2.0 \times 10^{31}$ and the detector is at position-1.

Event category	Trigger rate (Hz)	DAQ rate (Hz)	DAQ efficiency	$T_{10^8 coll}$ (sec)	N_{1h}
Single	18k	800	0.044	2,300	2.9M
(photon	10k	440			1.6M)
(neutron	8k	360			1.3M)
Type-I π^0	57	57	1.0	100	0.21M
Single (high-E γ)	500	500	1.0	100	1.8M

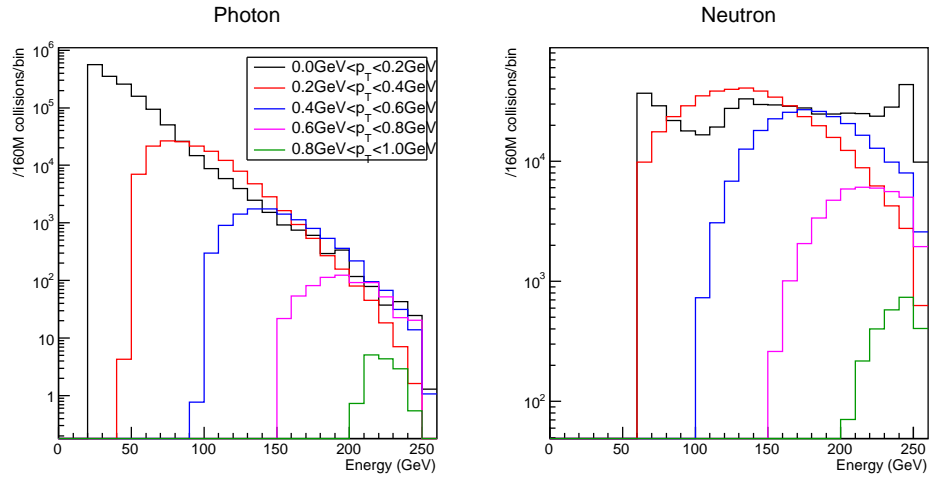


Figure 9: Expected observed spectra of single events after 1 hour (160M effective collisions) at the detector position-1.

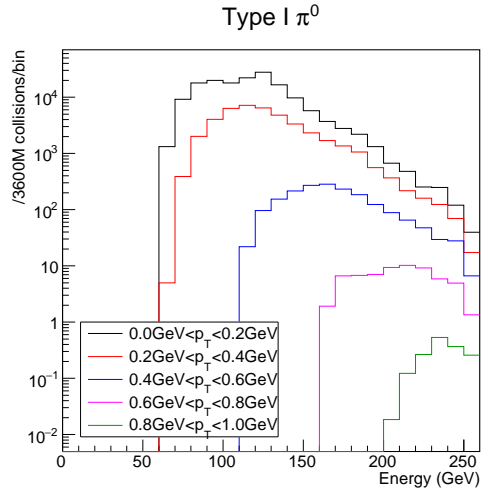


Figure 10: Expected observed spectra of Type I π^0 after 1 hour (3,600M collisions) at the detector position-1.

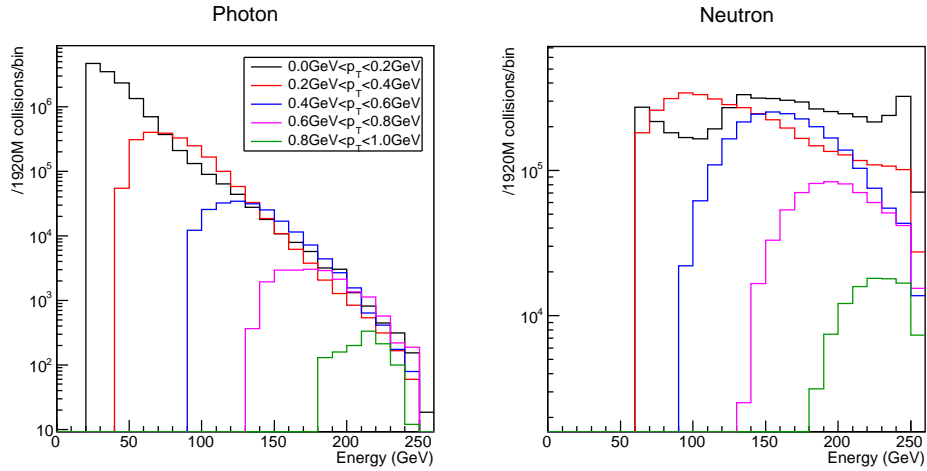


Figure 11: Expected observed spectra of single events after 12 hours (2040M effective collisions) at the detector positions-1, 2, 3.

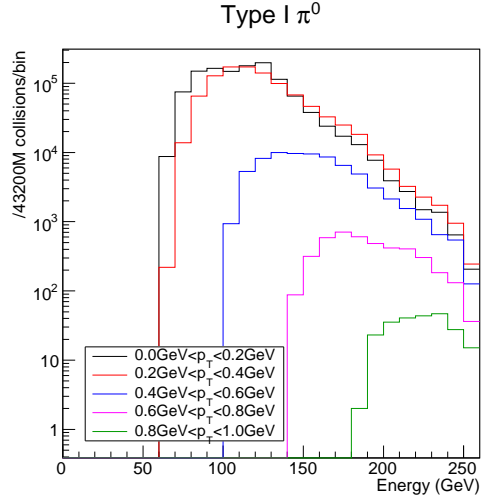


Figure 12: Expected observed spectra of Type I π^0 after 12 hours (43,200M collisions) at the detector positions-1, 2, 3.

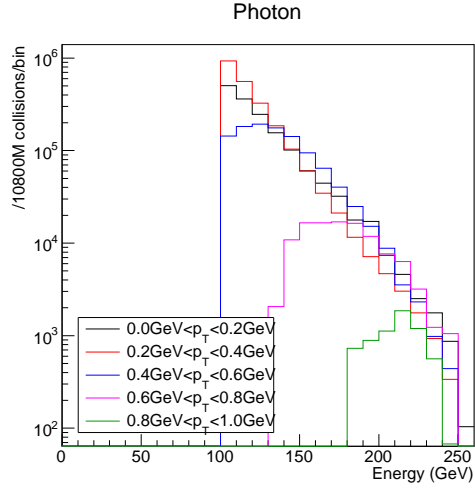


Figure 13: Expected observed spectra of high energy photon events after 3 hours (10,800M effective collisions) at the detector positions-1, 2, 3.

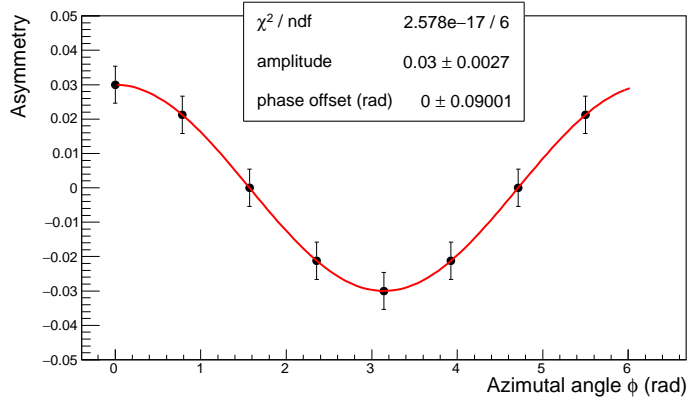


Figure 14: ϕ dependent asymmetry measurement using the 4 hours data of the small calorimeter at the position-1.

4.2.2 Asymmetry measurements

Number of neutrons (N) observed in the 12 hours of operation at the positions-1, 2 and 3 with standard trigger condition is summarized in Tab.4 for different p_T ranges. Statistical accuracy of asymmetry measurement $\delta A = 1/P\sqrt{N}$ is also listed, where polarization $P=50\%$ was assumed. Up to $p_T=1$ GeV, asymmetry A can be determined with $<1\%$ accuracy. This means the measurement of single-spin asymmetry can be performed in parallel with the cross section measurement.

Because the large calorimeter covers only a small fraction in azimuthal angle ϕ , actual direction of the polarization vector must be determined by the small calorimeter when the detector is at the position-1. Number of neutrons observed in the $3\text{ mm} < r < 8\text{ mm}$ ring region in the small calorimeter during 4 hours operation at the position-1 is 1.1×10^6 . In this case $\delta A=0.0019$ is expected. Average p_T of these neutrons close to zero degree is about 0.05 GeV. According to the PHENIX measurement and possible p_T scaling, there is still 2-3% asymmetry. Expected ϕ dependent asymmetry measurement in 4 hours of data taking at the position-1 is shown in Fig.14 assuming the amplitude of asymmetry to be 0.03. Under this assumption, the direction of polarization vector can be determined with an uncertainty of 0.09 radian (5.2°).

At the same time the large calorimeter records 3.2×10^6 neutrons with average p_T of 0.3 GeV. As shown in Fig.15, the ϕ coverage of the large calorimeter is only $\pm 15^\circ$. Expected ϕ dependent asymmetry measurement in 4 hours of data taking at the position-1 is shown in Fig.16 assuming the amplitude of asymmetry to be 0.12. Under this assumption, the direction of polarization vector can be determined with an uncertainty of 0.23 radian (13°).

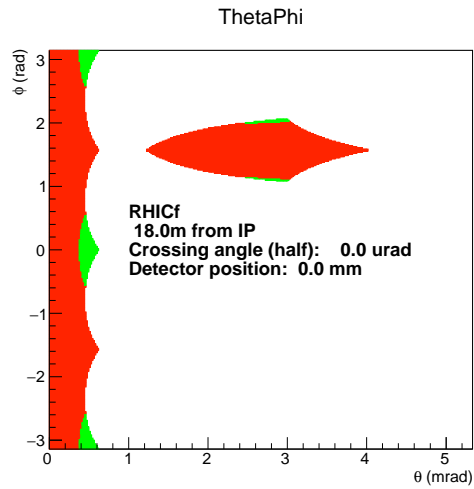


Figure 15: Angular coverage of the two calorimeters at the position-1. Red area shows the coverage for photon events while red+green shows the coverage for neutron events. Difference is due to the attenuation in the beam pipe. $\phi=\pi/2$ is the azimuthal direction to the vertical.

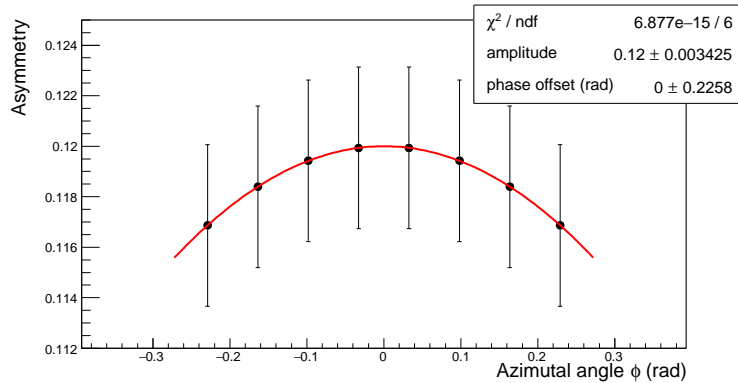


Figure 16: ϕ dependent asymmetry measurement using the 4 hours data of the large calorimeter at the position-1.

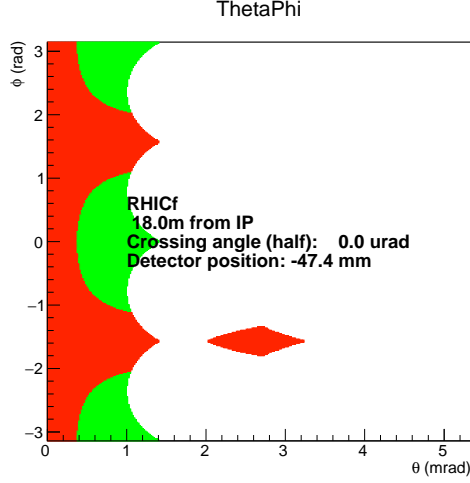


Figure 17: Angular coverage of the two calorimeters at the position-4. Red+green area shows the coverage for neutron events. Maximum asymmetry is expected along $\phi=0$ in case of the vertical polarization.

4.2.3 Backup plan of the asymmetry measurements

The key to perform a successful measurement in single-spin asymmetry is to use radially polarized beams. A backup plan in case there is any difficulty in the rotation of the polarization direction is discussed here. In case of vertical polarization, maximum asymmetry appears in the horizontal direction. To maximize the horizontal acceptance of the detector, the detector position-4 defined in Fig.8 is most effective. The angular coverage for the neutron events at this position is shown as 'red+green' area in Fig.17. Because the maximum asymmetry is expected along $\phi=0$, $\theta < 1$ mrad is covered. In 4 hours of data taking, 1.8×10^6 , 5.2×10^6 and 1.3×10^6 neutrons are observed in the p_T ranges, 0–0.1 GeV, 0.1–0.2 GeV and 0.2–0.3 GeV, respectively. Above 0.3 GeV, number of events drops quickly. Events fell within 3mm from the center are not counted here. The measurement is sufficient to determine the p_T dependence in asymmetry amplitude below 0.3 GeV, so that RHICf can test the result of PHENIX. Drawback is no sensitivity to the higher p_T over 0.3 GeV, where the evolution of amplitude is of great interest.

4.2.4 Summary

In summary to achieve our original physics goal, the data taking time below are required.

- 4 hours at positions-1, 2 and 3 (standard trigger), total 12 hours, is needed to achieve the minimal goal, that includes cross section measurements, single-spin asymmetry

measurement, and confirmation of the spin direction in parallel.

- 1 hour at 3 positions, total 3 hours, to increase the number of events for high-energy and high- p_T photons.
- 5 hours for surveys to understand the systematics such as trigger threshold, beam-gas background, beam pipe background, by changing the trigger condition, detector positions and the crossing angle.

In total, RHICf needs to be assured at least 24 hours of data taking time. Including the machine downtime and a moderate contingency in this tight plan, RHICf requires 48 hours for physics run.

In case there is any problem in the rotation of the polarization direction, using the vertical polarization excellent measurement of asymmetry in $p_T < 0.3$ GeV is possible. In this case asymmetry measurement about $p_T = 0.3$ GeV is not possible.

4.3 Joint analysis with STAR

As discussed in Sec.4.1, $\mu = 0.127$ in the above beam condition is not ideal for common physics analysis with STAR. To identify common collision between RHICf and STAR, lower pileup condition, $\mu \sim 0.01$ is required. An example of possible joint analysis is shown in Fig.18. Here photon and neutron spectra expected by the RHICf small calorimeter were simulated by PYTHIA 8212. Number of inelastic collisions was assumed to be 10^7 . The purple histograms are the spectra expected by the RHICf observation while the black and red show the breakdown of the event according to the origin as non-diffractive and diffractive, respectively. Interestingly, the contribution from two different categories of fundamental process is almost equal to such forward particle production. Though the simulation is on going, by requiring an existence of charged particles in the central region, the non-diffractive events are strongly enhanced. If the luminosity is reduced to 10% of maximum, collisions rate of 10^5 Hz (1.8 kHz RHICf trigger rate and 50% DAQ efficiency) and $\mu = 1\%$ is realized. Data equivalent to 10^7 collisions can be collected in 200 sec. Event selection with BBC and roman pot detectors will be sensitive to various ranges of diffractive masses. When the main RHICf targets are achieved within an approved time, a few hours of low luminosity ($\mu \sim 0.01$) run is also requested.

4.4 Beam setup time and contingency

Beam setup time to the requested optics was summarized in "RHIC Collider Projections (FY2014–FY2018)." It is confirmed that this estimate is valid for Run17. In summary,

- 1 day for high β^* setup
- 1-3 shifts to change the polarization direction from vertical to radial

Table 4: Number of neutrons and statistical accuracy to determine the asymmetry obtained in 12 hours of operation at positions-1, 2 and 3.

$p_T(\text{GeV})$	$N (\times 10^3)$	δA
0.0–0.1	2,310	0.0013
0.1–0.2	2,570	0.0012
0.2–0.3	1,710	0.0015
0.3–0.4	2,190	0.0014
0.4–0.5	1,210	0.0018
0.5–0.6	1,130	0.0019
0.6–0.7	402	0.0032
0.7–0.8	260	0.0039
0.8–1.2	104	0.0062

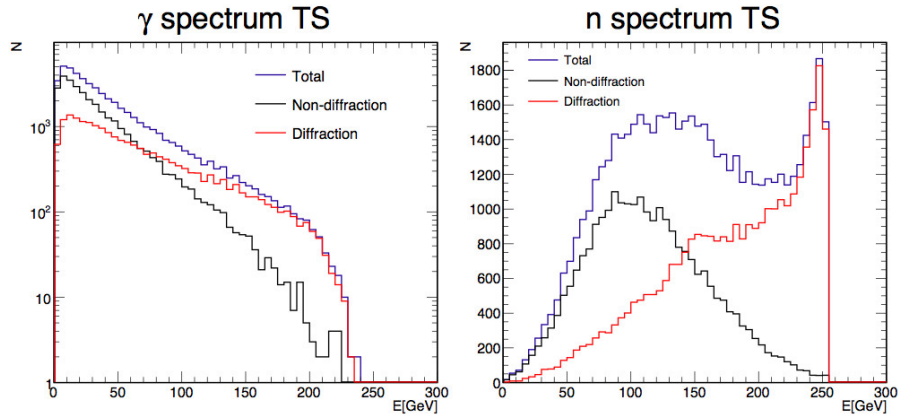


Figure 18: RHICf expected spectra in the small calorimeter at position-0.

According to these estimates, 2 days of beam setup are assumed.

Because the radial polarization with 255 GeV beam is the first attempt at RHIC, fast determination of the polarization direction is an issue of discussion. During this setup, the RHICf detector will be moved to the *garage* position to avoid interference to the ZDC. ZDC data will be used to confirm the direction of polarization. Inclination of $\pm 30^\circ$ from the ideal radial polarization results a reduction of asymmetry by a factor $\cos(30^\circ)=0.87$. This does not affect to the sensitivity of the RHICf measurement. As discussed in Sec.4.2.2, offline analysis of the RHICf data can improve the measurement of the polarization angle. Discussion for the actual procedure of this quick analysis is started between the STAR and RHICf collaborations.

The determination of the residual longitudinal polarization is difficult. Our measured amplitude of asymmetry will be normalized to the past measurements by PHENIX at $p_T=0.2-0.4$ GeV in $\sqrt{s}=500$ GeV collision. This does not affect the study of p_T scaling.

References

- [1] The RHICf Collaboration, arXiv:1401.1004.
- [2] The RHICf Collaboration, arXiv:1409.4860.
- [3] The LHCf Collaboration, Technical Design Report, CERN-LHCC-2006-004 (2006).
- [4] The LHCf Collaboration, Phys. Lett. **B715**, 298-303 (2012).; The LHCf Collaboration, Phys. Lett. **B703**, 128-134 (2011).; The LHCf Collaboration, Phys. Rev. **D86**, 092001 (2012).; The LHCf Collaboration, Phys. Lett. **B750**, 360-366 (2015).
- [5] The LHCf Collaboration, arXiv:1507.08764v2 [hep-ex]
- [6] K. Werner, F.-M. Liu, T. Pierog, *Phys. Rev. C* **74**, 044902 (2006).
- [7] T. Mase et al., Nucl. Instrum. Meth., **A671** 129-136 (2012).
- [8] B. Z. Kopeliovich, I. K. Potashnikova, I. Schmidt and J. Soffer, Phys. Rev. D **84**, 114012 (2011).
- [9] The PHENIX Collaboration, J. Phys. Conf. Ser., **295**, 012097 (2011).
- [10] C. Adler et al., Nucl. Instr. and Meth., **A499**, 433-436 (2002).
- [11] K.Kawade et al., JINST, **9**, P03016 (2014).
- [12] The LHCf Collaboration, JINST, **3**, S08006 (2008).
- [13] T. Suzuki et al., JINST, **8**, T01007 (2013).
- [14] The LHCf Collaboration, IJMPA, **28**, 1330036 (2013).